PHYSICAL REVIEW B VOLUME 27, NUMBER 3 1 FEBRUARY 1983

Superconductivity and the electronic structure of Zr- and Hf-based metallic glasses

M. Tenhover
Department of Research and Development, Warrensville Research Center, The Standard Oil Company (Ohio), 4440 Warrensville Center Road, Warrensville Heights, Ohio 44128

W. L. Johnson
W. M. Keck Laboratory of Engineering Materials, California Institute of Technology, Pasadena, California 91125

(Received 3 May 1982)

The results of a comprehensive study of the superconducting transition temperatures of Zr- and Hf-based metallic glasses are reported. The microscopic origins of superconductivity in these glasses are discussed in terms of recent ultraviolet photoelectron spectroscopy (UPS) measurements and calculations based on the renormalized atom technique. These calculations accurately predict the UPS spectra and the results of low-temperature heat-capacity measurements. The complete description of the electronic structure afforded by these calculations allows, for the first time, a consistent picture of the variation of T_c with X in the glasses $Zr_{1-y}X_y$ ($X=3d$ or $4d$ transition metals). In addition, the dependence of T_c with composition (y) can be understood in terms of the X d subband positions relative to E_F. The results reported here support our recent contention that the strong depression of T_c observed for $X=$Fe, Mn, Cr, and V glasses is related to the formation of localized magnetic moments and spin fluctuations. An alternate explanation for the low T_c of $X=$V and Cr glasses based on the idea of an atomic-structure change is also discussed.

INTRODUCTION

Metallic glasses of the form $Zr_{1-y}X_y$ have been the special focus of research in superconductivity[1-5] and the electronic structure of amorphous metals.[5-8] In part, the interest in this category of glasses stems from the variety of elements that can perform the role of X and the sometimes wide range of composition (y). In the present work metallic glasses in which X is a $3d$ or $4d$ transition metal are considered and a comprehensive study of the dependence of the superconducting transition temperature (T_c) on X is reported.

Superconductivity in amorphous metals is often discussed in terms of the number of electrons per atom (e/at.), treating this quantity as a fundamental parameter relating T_c and the amorphous alloy. It will be shown that this approach is inadequate and that the superconducting properties and photoemission results on the Zr-based glasses can best be understood when explicit account is taken of the d subbands associated with the components of the glass. A simple method of understanding and predicting the electronic structure of transition-metal glasses based on the renormalized-atom approach[9] is developed. This approach is shown to provide qualitative agreement with the available photoemission results and quantitative agreement with experimental determinations of the density of electronic states at the Fermi level. These results are used to provide the framework for a microscopic understanding of the origins of superconductivity in these glasses. In particular, the dependence of T_c on alloy identity (X) and composition (y) in Zr-based amorphous alloys can be explained. Also, support is found for the recent suggestion[5] that the depression of T_c observed for $X=$Co, Fe, Mn, Cr, and V glasses is related to the formation of localized magnetic moments and spin fluctuations.

EXPERIMENTAL

Alloys of $Zr_{70}X_{30}$ and Hf-X were prepared by levitation melting of the components in a Ti-gettered Ar atmosphere. The starting materials were at least 99.99% pure. Rapidly quenched foils were prepared with the use of the splat cooling technique in a flowing He atmosphere.[10] The composition of the splat-quenched foils was checked by x-ray fluorescence measurements. Careful x-ray diffraction scans (rate of $0.02°\,\mathrm{min}^{-1}$) using Cu $K\alpha$ radiation were taken of the as-quenched foils. Those foils that showed a

TABLE I. Superconducting and normal-state resistivity values for $Zr_{70}X_{30}$ metallic glasses.

X	T_c (k)	dH_{c2}/dT (T/K)	ρ(300 K) ($\mu\Omega$ cm)
Cu	2.7	2.67	165
Ni	2.8	3.09	180
Co	3.2	3.32	145
Fe	1.9	3.43	148
Mn	<1.2		140
Cr	<1.2		
V	1.3		
Pd	2.5	2.65	180
Rh	4.4	2.90	150
$Co_{0.5}Ni_{0.5}$	2.9		
$Ni_{0.5}Fe_{0.5}$	2.2		
$Mn_{0.5}Fe_{0.5}$	<1.2		
$Ni_{0.66}V_{0.34}$	2.8		

smooth featureless band in the x-ray scans were classified as amorphous. The following completely amorphous $Zr_{70}X_{30}$ foils were prepared: X=Cu, Ni, Co, Fe, Mn, Cr, V, Pd, Rh, $Co_{0.5}Ni_{0.5}$, $Fe_{0.5}Ni_{0.5}$, $Mn_{0.5}Fe_{0.5}$, and $Ni_{0.66}V_{0.34}$. In addition, amorphous foils of $Hf_{60}V_{40}$, $Hf_{70}Fe_{30}$, $Hf_{70}Ni_{30}$, $Hf_{72}Pd_{28}$, and $Hf_{80}Pt_{20}$ were prepared. In the case of X=V it was necessary to increase the V content (i.e., $Zr_{64}V_{36}$) to obtain good glassy samples. All measurements reported here are on materials that appeared from x-ray diffraction scans to be completely amorphous. The superconducting transition temperature (T_c), and for some samples the perpendicular upper critical magnetic field [$H_{c2}(T)$], were measured resistively with the use of a standard four-point probe down to a temperature of 1.2 K.

EXPERIMENTAL RESULTS

The results of the T_c and $H_{c2}(T)$ measurements are summarized in Tables I and II and Fig. 1. For X=Cu, Ni, Co, Pd, Rh, and $Ni_{0.66}V_{0.34}$, and for $Hf_{70}Ni_{30}$, $Hf_{72}Pd_{28}$, and $Hf_{80}Pt_{20}$, very sharp superconducting transitions ($\Delta T_c < 0.05$ K) were observed. In the X=Fe and $Ni_{0.5}Fe_{0.5}$ samples the transition width was relatively broad ($\Delta T_c > 0.15$ K). This may indicate that these samples are not homogeneous or, despite the x-ray diffraction evidence, not completely amorphous. Karput and Hake[11] have reported that the T_c of $Zr_{70}Fe_{30}$-quenched ribbons is less than 1.2 K. The reason for this discrepancy is not clear and is perhaps related to sample preparation methods; for now it seems safe to assume that the T_c of $Zr_{70}Fe_{30}$ reported here (1.90 K) is an upper bound.

Starting with X=Cu and moving to Ni and Co, a gradual increase in T_c is observed. In Ref. 12 the T_c of amorphous Zr_3Ag was reported to be 2.3 K. Combining this with the X=Pd and Rh data, the same trend for T_c that was observed for the 3d elements emerges; however, the rate of increase is noticeably larger. In the $X=3d$ series a strong depression of T_c is observed for the elements to the left of Co. The T_c values of the $X=Mn_{0.5}Fe_{0.5}$, Mn, and Cr glasses are below 1.2 K. At X=V superconduc-

TABLE II. Transition temperatures for Hf-based glasses.

Alloy	T_c (K)
$Hf_{60}V_{40}$	<1.2
$Hf_{70}Fe_{30}$	<1.2
$Hf_{70}Ni_{30}$	1.5
$Hf_{72}Pd_{28}$	1.3
$Hf_{80}Pt_{20}$	1.4

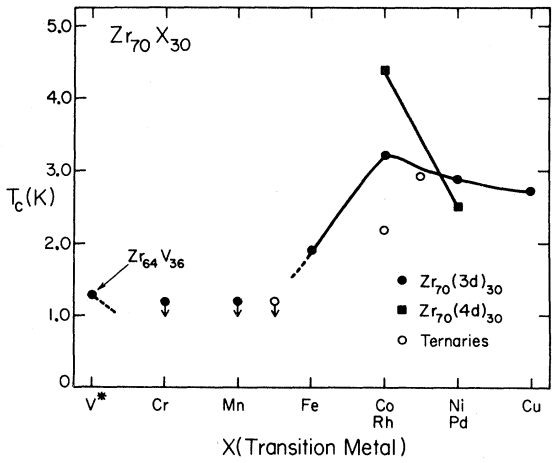

FIG. 1. Results of T_c measurements on $Zr_{70}X_{30}$ metallic glasses. Downward-pointing arrows on some of the points indicate that T_c is less than 1.2 K.

tivity reappears, although the T_c is still quite low. There is no available information concerning T_c of X=Nb, Mo, Tc, or Ru metallic glasses. From Collver and Hammond's work on cryogenically deposited thin films of transition metals[13] we can roughly estimate the T_c of amorphous Zr (T_c=3.0 K), $Zr_{70}Nb_{30}$ (T_c=4.0 K), and $Zr_{70}Mo_{30}$ (T_c=5.0 K). From this information and the X=Ag, Pd, and Rh data, T_c appears to increase as X moves to the middle of the 4*d* row and a maximum value of T_c is expected to occur near X=Tc or Ru. The behavior of the 4*d* series is in sharp contrast to that of the 3*d* additions.

The dependence of T_c on composition for the ternary glasses is particularly interesting and revealing. The $X=Co_{0.5}Ni_{0.5}$ glass has a T_c that falls slightly below the line connecting the X=Co and Ni glasses. In the $X=Ni_{0.66}V_{0.34}$ glass the replacement of a third of the Ni in the X=Ni glass by V does not change T_c significantly. Despite having the same value of e/at. as the X=Co glass, the $X=Ni_{0.5}Fe_{0.5}$ glass is found to have a considerably lower T_c. From the limited data on the Hf-based glasses in Table II it is clear that T_c is lower for the Hf-X glass than the corresponding Zr glass. However, the same trend with X identity emerges as the Hf-Ni glass has a higher T_c than both the Hf-Pd and Hf-Fe glasses.

The upper critical magnetic field [$H_{c2}(T)$] was measured as a function of T for X=Cu, Ni, Co, Fe, $Ni_{0.5}Fe_{0.5}$, Pd, and Rh. Near T_c the $H_{c2}(T)$ curves were linear permitting a determination of the field gradient. A more detailed report on the $H_{c2}(T)$ measurements and flux pinning measurements in the X=Co, Ni, $Ni_{0.5}Fe_{0.5}$, and Fe samples is planned to be given.[14]

From the field-gradient measurements and the normal-state resistivity the density of electronic states at the Fermi level can be estimated from the relation[15]

$$D(0)=\left[\frac{\pi^2\hbar}{8e^2k_B\phi_0\rho}\right]\left.\frac{dH_{c2}}{dT}\right|_{T_c},$$

where ϕ_0 is the fundamental flux quantum. The $D(0)$ values are listed in Table III and are compared to those obtained from low-temperature heat-capacity measurements. The agreement between the two determinations of $D(0)$ is excellent. This same level of agreement has been observed in a wide variety of metallic glass superconductors.[16] A clear correlation exists between the values of $D(0)$ and T_c. With the exception of X=Fe and Co, a higher $D(0)$ corresponds to a high T_c. The X=Co case is not a serious discrepancy in that its $D(0)$ and T_c are higher than X=Cu, Ni, and Pd. In the next section emphasis will be placed on the relation between T_c and $D(0)$, and it will be shown that this is the key to understanding superconductivity in these materials.

TABLE III. Dressed density of states from heat-capacity and critical-field measurements.

X	$D^*(0)$ (states/eV atom spin) (critical field)	$D^*(0)$ (states/eV atom spin) (heat capacity)
Cu	0.90	0.85
Ni	1.06	
Co	1.41	
Fe	1.43	
Pd	0.96	1.00
Rh[a]	1.22	1.20

[a]For Zr_3Rh.

DISCUSSION

In Ref. 16 the authors have discussed the microscopic origin of superconductivity in metallic glasses and have related it to the electronic structure of metallic glasses. The starting point for a discussion of this nature is McMillan's approximate solution to the Eliashberg equations,[17]

$$T_c=\frac{\langle\omega\rangle}{1.45}\exp\left[\frac{-1.04\lambda}{\lambda-\mu^*(1+0.62\lambda)}\right],$$

where λ is the electron-phonon coupling constant, μ^* is the effective Coulomb coupling constant for electron repulsion, and $\langle\omega\rangle$ is the average phonon frequency. The electron-phonon coupling constant can be expressed as

$$\lambda=\frac{D(0)\langle I^2\rangle}{M\langle\omega^2\rangle_m},$$

where $\langle I^2\rangle$ is the square of the electronic matrix element associated with the change in crystal potential as an atom is moved and $\langle\omega^2\rangle_m$ is the average squared phonon frequency defined by McMillan.[17] Varma and Dynes[18] have derived the approximate relation $\lambda=D(0)\delta$, where $\delta=\langle I^2\rangle/M\langle\omega^2\rangle$ should be roughly constant for transition-metal alloys of a given series. In Fig. 2, from Ref. 16, the validity of the Varma-Dynes relation is demonstrated for the amorphous alloys Zr-Pd, Zr-Rh, Zr-Cu, $Mo_{1-x}Ru_x$, and Nb_3Ge and crystalline bcc alloys of Nb, Zr, Mo and Tc. The data fall on two values of δ depending on whether the states at the Fermi energy E_F lie in the lower half (bonding) or upper half (anitbonding) of the 4*d* band. To a good approximation λ can be taken as a simple function of $D(0)$ for amorphous and crystalline materials in which the states at E_F

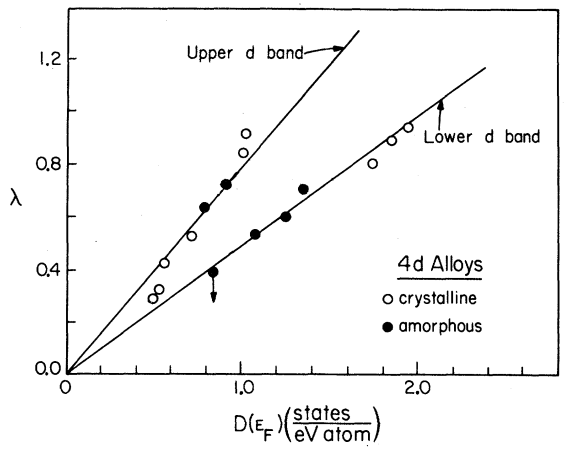

FIG. 2. Electron-phonon coupling parameter plotted as a function of the density of states at the Fermi energy for crystalline and amorphous alloys based on 4*d* transition metals.

are primarily 4*d* orbitals. In principle, knowledge of $D(0)$ permits the calculation of λ and therefore of T_c.

From the discussion above it is clear that a comprehensive description of superconductivity in the Zr-based glass requires information on $D(E)$ for each alloy. At present, low-temperature heat-capacity data are available for Zr-Cu,[3] Zr-Rh,[19] and Zr-Pd,[20] while photoemission spectra have been reported for Zr-Cu, Zr-Pd,[6] Zr-Ni, Zr-Co,[7] and Zr-Fe.[8] To complete the description of the electronic structure of the Zr glasses a simple theoretical method for predicting $D(E)$ is now developed.

The chemical and topological disorder inherent in an amorphous material makes the determination of the electronic structure especially difficult. There are two common approaches to this problem. One is to use the atomic coordinates of hard-sphere or computer-generated models to perform a tight-binding analysis for a finite number of atoms.[21,22] The other approach is to carry out a cluster calculation assuming that a finite number of local geometrics occur in the amorphous structure.[23,24] The present approach is to determine the atomic-structure–independent features of the electronic spectrum with the use of the concept of the renormalized atom.

The renormalized-atom approach was first used by Chodorow[25] and Segall[26] for crystalline Cu metal and was later extensively developed by Hodges *et al.*[9] for 3*d* and 4*d* transition metals. In this approach, free-atom *s* and *d* wave functions are used which have been truncated at the radius of the Wigner-Seitz sphere and renormalized within this sphere. This renormalization prepares the atoms in approximately the condition in which they exist in the solid. Using the definition of the renormalized wave functions above, Hodges *et al.*[9] have shown how to construct renormalized-atom potentials and calculate *d*-band centroids and bandwidths. By allowing the renormalization to account for the two Wigner-Seitz cell volumes appropriate to each component, it becomes possible to treat the binary alloy case. The results of the renormalized-atom calculation for the atoms of interest are displayed in Table IV. They are in good agreement with the values reported by Ref. 9 in Figs. 5, 6, and the bottom of Fig. 8. The renormalized-atom energies and bandwidths provide good estimates for the centroids and widths of each separate subband. Because of the large degree of disorder in the atomic structure of these alloys it is reasonable to assume that the separate subbands are relatively featureless. For convenience, the shape of each *d* subband is taken to be Lorentzian. No physical significance is associated with this choice of the subband shape, and other shapes might be more appropriate. In particular, the form suggested by Hubbard[27] could also be used. The important approximation is the use of a symmetric subband shape. A complete coherent-potential (CP) calculation would be required to determine the compositional dependence of the subband widths for the alloys of interest.[28] For simplicity, the dependence of the subband width with composition is determined by the relation derived by Velicky *et al.*[28] for the dilute split-band limit, namely that the subband width should vary as the square root of composition. This amounts to a scaling of the Zr subband width by (0.83) and the *X*-subband widths by (0.55) for the alloys $Zr_{70}X_{30}$. Using this approximation for the

TABLE IV. Results of renormalized-atom calculations of *d*-band centroids (E_d) and bandwidths (W_d).

Transition metal	E_d (eV)	W_d (eV)
Zr	−0.9	8.5
Cu	−5.8	3.7
Ni	−4.3	4.7
Co	−3.3	5.4
Fe	−2.4	6.5
Mn	−1.3	7.4
Cr	−0.2	8.4
V	−0.2	8.1
Ag	−8.9	4.2
Pd	−6.2	6.6
Rh	−3.9	8.5
Ru	−2.6	10.4
Tc	−2.0	10.7
Mo	−1.0	11.0
Nb	−0.8	10.4

case of overlapping subbands leads to an underestimate of the subband width. Likewise, the use of a single Wigner-Seitz radius for each element also results in an underestimate of the effective subband widths. A more realistic approach might be to use a distribution of Wigner-Seitz radii to account for the range of interatomic spacings observed in amorphous alloys. For each value of the Wigner-Seitz radius, a different value of the average subband energy will result. This of course means that the actual d subband will be broader than that predicted by the use of a single Wigner-Seitz radius. This effect, plus the failure to take into account the CP corrections to the subband widths in the cases of overlapping subbands, means that the widths used in the present calculations should be considered as lower limits to the actual widths. As will be mentioned later, this underestimate of the subband widths will result in an overestimate of $D(0)$ for the amorphous alloys. The purpose of the present work is to understand the gross features of the electronic structure of the Zr-based glasses, without input on the details of the atomic structure. In this spirit the simple treatment of the subband positions and widths described here is appropriate. The contributions of s states to $D(E)$ is expected to be small and is ignored here. Furthermore, s-d hybridization is neglected and the elements are assumed to have either the $3d^{N-1}4s^1$ or $4d^{N-1}5s^1$ (N is the total number of conduction electrons) configuration. No attempt is made to account for charge-transfer effects or level repulsion due to band formation.[28]

The projected density-of-states plots for some Zr $3d$ and Zr $4d$ alloys are shown in Figs. 3 and 4. The density-of-states scale is determined by requiring the subbands to contain a total of the ten electron states per atom. Likewise, the Fermi level is found by requiring the occupied electronic states to contain the proper number of d electrons for each alloy. The $D(E)$ plots are in excellent agreement with existing ultraviolet photoelectron spectroscopy (UPS) and x-ray photoelectron spectroscopy (XPS) data.[6–8] The nature of the photoemission spectra and the dramatic changes that occur as X is varied can be readily explained. In Fig. 3, starting with X=Cu, the two distinct peaks in the spectrum represent contributions primarily from Zr $4d$ (centered at about $+2$ eV) and Cu $3d$ (centered at about -2.8 eV). This alloy is a classic example of the split-band limit.[28] Moving to the left in the $3d$ row, the renormalized energy levels of the $3d$ component approach those of Zr until at Fe and Mn the two subbands completely overlap. The glasses X=Fe and Mn are, therefore, examples of the virtual-crystal limit.[28] Similar behavior is observed for the Zr $4d$ alloys (Fig. 4). The displacements (Δ) of the

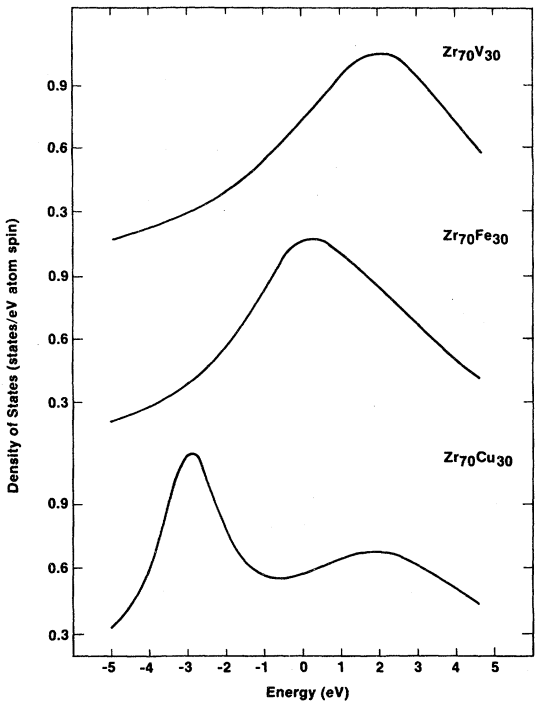

FIG. 3. Predicted density of electronic states has a function of energy for several Zr $3d$ glasses.

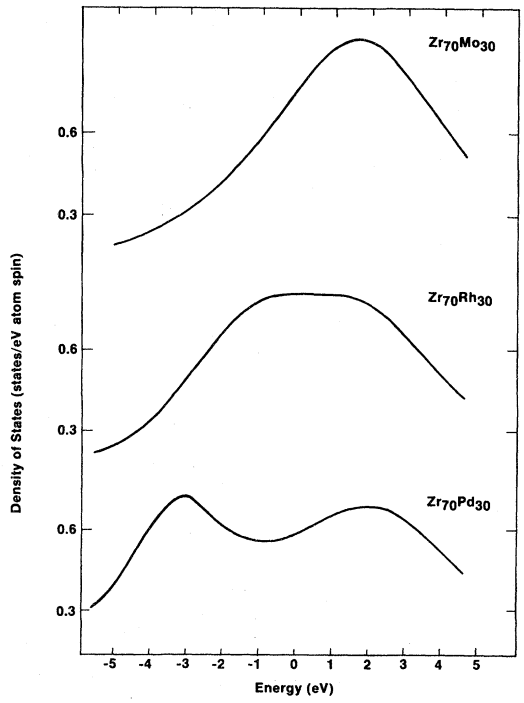

FIG. 4. Predicted density of electronic states as a function of energy for several Zr $4d$ glasses.

3d and 4d subband positions from the Fermi energy (E_F) are listed in Table V and compared to the experimental data. The agreement between the experimental values and the predicted values is quite good. The values also provide a convenient parameter for describing the nature of the electronic states near E_F. For example, the large negative value for X=Ag means that the Ag 4d states are far below E_F and make very little contribution, while the small value of Δ for X=Fe indicates that the Fe 3d subband is roughly centered at E_F and that these states play an important role in determining the properties of the alloy.

From the projected $D(E)$ functions, the density of states at the Fermi energy [$D(0)$] can be determined and these values are listed in Table VI. For comparison, the dressed $D(0)$ values from low-temperature heat-capacity experiments have been converted to bare density of states using the λ values: Cu(0.53), Pd(0.60), and Rh(0.71).[29] The good agreement obtained here encourages the use of the calculated $D(0)$ values in the discussion of superconductivity in the materials. In Fig. 5 the calculated values of $D(0)$ are plotted for the Zr 4d amorphous alloys along with the T_c values from Table I. The broad maximum in the $D(0)$ curve is primarily the result of the X-component subband lining up with the Fermi energy, as is evident upon comparing Table V and Fig. 5. The height of this maximum is of course dependent on the choice of the subband widths. In particular, narrow X-subband widths will give a sharper maximum in $D(0)$. The neglect of the CP corrections to the subband widths in the overlapping subband cases and the use of a single Wigner-Seitz radius does affect the details of the $D(0)$ curve in Fig. 5. However, the basic character of the $D(0)$ vs X curve should remain the same since it is primarily the result of the X subband position relative to the Fermi energy. In the discussion below, the Varma-Dynes relation will be used to relate $D(0)$ and T_c. Strictly speaking, an extension of this idea is needed to treat the cases of different subband widths and types of orbitals (3d or 4d). In the

TABLE V. Positions of the X d subbands relative to E_F from theory (Δ_{theor}) and experiment (Δ_{expt}) for $Zr_{70}X_{30}$ glasses.

X	Δ_{theor} (eV)	Δ_{expt} (eV)
Cu	−2.96	−3.4
Ni	−1.70	−1.9
Co	−0.85	−1.4
Fe	−0.15	0.0
Mn	+0.45	
Cr	+1.82	
V	+2.20	
Ag	−6.00	
Pd	−3.30	−3.4
Rh	−1.40	
Ru	−0.31	
Tc	+0.41	
Mo	+1.40	
Nb	+1.96	
Zr	+2.50	

TABLE VI. Density of states at E_F of $Zr_{70}X_{30}$ metallic glasses from theory and experiments.

X	$D(0)_{theor}$ (states/eV atom spin)	$D(0)_{expt}$ (states/eV atom spin)
Cu	0.58	0.56
Ni	0.78	
Co	1.01	
Fe	1.07	
Mn	1.04	
Cr	0.83	
V	0.75	
Ag	0.50	
Pd	0.59	0.63
Rh	0.82	0.70[a]
Ru	0.87	
Tc	0.85	
Mo	0.78	
Nb	0.71	
Zr	0.60	

[a]For Zr_3Rh.

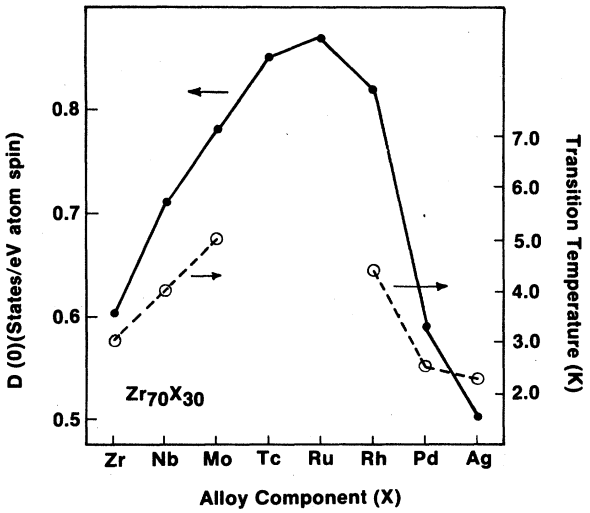

FIG. 5. Predicted density of electronic states at the Fermi energy for Zr 4d amorphous alloys (solid circles) and the experimental values of T_c (open circles). For X=Zr, Nb, and Mo the T_c values are estimated from Ref. 12, and for X=Ag the T_c measurement is for amorphous Zr_3Ag.

absence of such an extension the discussion will be of a qualitative nature. On the left-hand side of Fig. 5 (X=Zr, Nb, and Mo) the states at E_F originate from 4d bonding states and the Varma-Dynes parameter (δ) is expected to be roughly constant. In this case λ is expected to be proportional to $D(0)$, which means that the increase in $D(0)$ directly translates into an increase in T_c. For the split-band glasses X=Pd and Ag the states at E_f are once again the 4d bonding states, this time originating primarily from only the Zr 4d subband. A similar relation between $D(0)$ and T_c is expected. For X=Tc, Ru, and Rh, the states at E_F have both a bonding and anitbonding character. This, plus the fact that the bandwidths of the two separate subbands are different, makes this a more difficult case to consider. The Varma-Dynes parameter (δ) is not constant here but probably varies from the values for the bonding and antibonding cases. A maximum in T_c for the Zr 4d glasses is thus expected to occur for X=Tc or Ru.

The $D(0)$ vs X curve for the Zr 3d glasses is very similar to that of X=4d materials. The values are listed in Table VI. The maximum $D(0)$ occurs in the region near X=Co, Fe, and Mn and is considerably higher than the maximum in the X=4d case. This is the result of the narrow bandwidths calculated for the 3d components compared to the 4d components. In the case of the split-band glasses X=Cu and Ni, the states at E_F originate primarily from the Zr 4d bonding orbitals. As discussed above for the X=4d glasses, T_c is expected to be related directly to changes in $D(0)$. Comparing the four split-band limit glasses (X=Ag, Pd, Cu, and Ni), T_c is found to follow nicely the trend of the calculated values of $D(0)$. Surprisingly, the large increase in $D(0)$ that results on moving from X=Ni to Co does not increase T_c much. The relatively high $D(0)$ values for X=Fe, Mn, and Cr also do not translate into high T_c values. It has been suggested that the unexpectedly low values of T_c for X=Co, Fe, Mn, and Cr are the result of the formation of spin fluctuations and localized magnetic moments.[5] The conditions for forming a localized moment are to have the intra-atomic Coulomb energy greater than the width of the 3d subband and to have the centroid of the 3d element less than a bandwidth away from E_F.[30] The Δ values from Table V clearly show that the second condition is satisfied for X=Co, Fe, Mn, and Cr, and since the intra-atomic Coulomb energy is roughly the same for all of these elements, magnetic moment formation is likely. This finding supports the claim that the mechanism depressing T_c in the 3d glasses is magnetic in origin. Other than the observed depression of T_c in the Zr 3d glasses, there is no reported experimental evidence for magnetic moment formation. Clearly, this is a very interesting area and hopefully some experimental support will be reported for the ideas discussed above.

The measured values of T_c for the ternary glasses X=$Co_{0.5}Ni_{0.5}$, $Ni_{0.5}Fe_{0.5}$, $Mn_{0.5}Fe_{0.5}$, and $Ni_{0.66}V_{0.34}$ provide additional insight concerning the formation of localized magnetic moments. In the X=$Co_{0.5}Ni_{0.5}$ case the observed increase in T_c that occurs as Ni is replaced by Co can be qualitively explained by the expected increase in the bare density of states $D(0)$. Although, like the X=Co glass, the increase in T_c is smaller than what would be expected for the predicted increase in $D(0)$, a similar increase in $D(0)$ is expected as Ni is replaced by Fe; however, a sharp drop in T_c is experimentally observed. This behavior is a clear example of a breakdown in the rigid-band model. The Fe levels resulting from the substitution of Ni fall at E_F and satisfy the conditions for forming localized magnetic moments. In fact, because of the relation between subband width and composition mentioned above, the tendency toward localized moment formation should actually be enhanced at low Fe concentrations. The pair-breaking ability and therefore the depression of T_c depend on both the magnitude and number of magnetic moments formed.[31] The T_c-versus-composition behavior will depend on the interplay of these two properties. One important factor to consider in deciding whether a given 3d element will form a moment in a metallic glass is the variety of local atomic environments available for the 3d element to occupy. Even if the average local atomic environment is unfavorable for moment formation, it may still be possible for some of the 3d atomic sites to satisfy the necessary requirements. This analysis leads to the important conclusion that the disordered atomic sturcture of amorphous alloys enhances the tendency of forming localized magnetic moments and spin fluctuations. In the 3d series it appears likely that Co, Fe, Mn, Cr, and perhaps V behave magnetically in Zr glasses. The final ternary system investigated was the Zr-Ni-V glasses. This ternary system was chosen for study because $D(0)$ is expected to be nearly constant across the Ni-V composition range. The X=$Ni_{0.66}V_{0.34}$ glass has a T_c (2.8 K) that is virtually identical to that of the pure X=Ni glass. This result is somewhat puzzling in light of the discussion above if it is assumed that V forms localized magnetic moments. The endpoint of the Zr-Ni-V series, X=V, has a much lower T_c than that of X=Ni. Clearly, a sharp decrease in T_c must occur at some V concentration.

An alternate explanation for the low T_c of the X=V and perhaps Cr glasses is that the higher moments of the $D(E)$ spectrum become important due to a change in the atomic structure. Evidence for

such an atomic-structure change has recently been observed in Mo-Ru-B glasses.[32] Here, an atomic-structure change is claimed to result in nearly a factor-of-2 drop in the electronic specific-heat coefficient. Johnson *et al.*[33] have noted a correlation between glass-forming ability and the occurrence of high-temperature superconductivity. They suggested that the softening of the crystalline lattice against harmonic displacements expected for a high-temperature superconductor and amorphous phase formation might be linked to a common mechanism, namely the polarization of the *d*-electron gas. Implicit in this discussion is the idea that the glass-forming ability is pronounced in regions of composition in which there is competition for stability between bcc and hcp crystalline phases. In the $Zr_{70}X_{30}$ materials studied here the difficulty in preparing glasses increases as X moves to the left of the Periodic Table. Attempts to prepare glasses of $Zr_{70}Ru_{30}$ have been unsuccessful, although a study of Zr-Ru-Rh and Zr-Ru-B glasses is planned to be reported.[34] The difficulty in preparing X=Ru glasses is believed to be due to an overwhelming tendency to form bcc solid solutions. In the $X=3d$ series the small metallic radii of these elements reduce the tendency to form bcc solutions and enhance the glass-forming ability. The difficulty in preparing X=V and Cr glasses may be a manifestation of a change in the local atomic structure to one having a predominate bcc-like character. A difference in short-range atomic structure has been reported for the related glasses $Y_{66}T_{34}$ depending on whether T=Cu and Zn or T=Ni, Co, Fe, and Mn.[35] The point of this discussion is to suggest the possibility that the low T_c of X=V and perhaps X=Cr may be due to a change in the atomic structure from closed packed to one having a bcc-like packing and low $D(0)$ instead of the formation of localized magnetic moments.

The electronic structure of the Hf glasses is expected to be very similar to that of the Zr-based glasses. The lower T_c for the Hf-X glasses results from the higher ionic mass of Hf compared to Zr and the resulting decrease in the Debye temperature. Like the case of the Zr 3*d* glasses, magnetic moment formation is likely to occur in the Hf 3*d* glasses.

A subject of some interest has been the compositional dependence of $T_c(dT_c/dy)$ in glasses of the form $Zr_{1-y}X_y$. The available experimental values are the following: X=Cu (0.095),[3] Pd (0.082),[2] and Zr-Ni(0.063).[4] A simple explanation for this behavior is suggested by the positions of the X subbands and the contribution they make to $D(0)$. In the case of X=Cu, as Zr is replaced by Cu, electronic states are transferred from the Zr 4*d* subband [where they contribute to $D(0)$] to the Cu 3*d* band [where they make almost no contribution to $D(0)$]. This transfer of states is expected to decrease T_c sharply. The X=Pd glasses are similar to the Cu case except that the larger bandwidth of Pd means that in replacing Zr by Pd the Pd states contribute somewhat to $D(0)$, thus reducing the value of dT_c/dy. Moving to X=Ni, the Ni subband is expected to make more of a contribution to $D(0)$ than Cu or Pd, thereby having the smallest value of dT_c/dy. Based on this reasoning, the compositional dependence of T_c is expected to be largest for glasses such as X=Ag and smallest for glasses such as X=Rh, Ru, and Tc. For cases in which X is expected to carry a localized magnetic moment, the compositional dependence of T_c will be larger than that predicted by the positions of the subbands relative to E_f.

Ultraviolet and x-ray photoemission experiments are in progress on the glasses X=V, Cr, and Mn. Preliminary results are in excellent agreement with the predicted $D(E)$ spectra. This work is planned to be reported in the near future.[36]

CONCLUSIONS

A comprehensive study of superconductivity in Zr- and Hf-based metallic glasses has been reported. The observed T_c values can be understood in terms of the electronic structure of the glasses. A simple method of calculating $D(E)$ with the use of the renormalized-atom approach was developed and shown to provide a useful basis for understanding and predicting the results of photoemission and low-temperature heat-capacity experiments. The conditions for formation of localized magnetic moment formation and spin fluctuations were examined and appear to be satisfied by the X=Co, Fe, Mn, and Cr glasses. An alternate explanation for the low T_c values of X=V and Cr involving an atomic-structure change was suggested. Finally, the composition dependence of T_c in $Zr_{1-y}X_y$ glasses was described in terms of the subband positions.

ACKNOWLEDGMENT

One of us (W.L.J.) received support from the U. S. Department of Energy, Project Agreement No. DE-AT03-81ER10870 under Contract No. DE-AM03-76SF00767.

[1]W. L. Johnson and S. J. Poon, J. Appl. Phys. 46, 1787 (1975).
[2]G. R. Gruzalski, J. A. Gerber, and D. J. Sellmyer, Phys. Rev. B 19, 3469 (1979).
[3]G. von Minnigerode and K. Samwer, Physica (Utrecht) 108B, 1217 (1981).
[4]E. Babic, R. Ristic, M. Miljak, M. G. Scott, and G. Gregan, Solid State Commun. 39, 139 (1981).
[5]M. Tenhover and W. L. Johnson, Physica (Utrecht) 108B, 1221 (1981).
[6]P. Oelhafen, E. Hauser, H. J. Guntherodt, and K. K. Bennemann, Phys. Rev. Lett. 43, 1134 (1979).
[7]A. Amamou and G. Krill, Solid State Commun. 28, 957 (1978).
[8]P. Oelhafen, E. Hauser, and H. J. Guntherodt, Solid State Commun. 35, 1017 (1980).
[9]L. Hodges, R. E. Watson, and H. Ehrenreich, Phys. Rev. B 5, 3953 (1972).
[10]Pol Duwez, *Progress in Solid State Chemistry* (Pergamon, Oxford, 1966), Vol. 3.
[11]M. G. Karkut and R. R. Hake, Physica (Utrecht) 109-110B, 2033 (1982).
[12]A. Ravex, J. C. Lasjaunais, and O. Bethoux, Physica (Utrecht) 107B, 395 (1981).
[13]M. M. Collver and R. H. Hammond, Phys. Rev. Lett. 30, 92 (1973).
[14]M. Tenhover (unpublished).
[15]D. Saint-James, G. Sarma, and E. J. Thomas, *Type II Superconductivity* (Pergamon, Oxford, 1969).
[16]W. L. Johnson and M. Tenhover, in *The Magnetic, Chemical, and Structural Properties of Glassy Metallic Alloys,* edited by R. Hasegawa (CRC, Boca Raton, 1982).
[17]W. L. McMillan, Phys. Rev. 167, 331 (1968).
[18]C. M. Varma and R. C. Dynes, *Superconductivity in d- and f-band Metals,* edited by D. H. Douglass (Plenum, New York, 1976).
[19]P. Garoche and W. L. Johnson, Solid State Commun. 39, 403 (1981).
[20]U. Mitutani, K. T. Hartwig, T. B. Massalski, and R. W. Hopper, Phys. Rev. Lett. 41, 661 (1978).
[21]T. Fujiwara, J. Phys. F 9, 2011 (1979).
[22]J. P. Gaspard, J. Phys. (Paris) 41, C8 (1980).
[23]G. Zwicknagel, Z. Phys. B 40, 31 (1980).
[24]B. Delley, D. E. Ellis, and A. J. Freeman, J. Phys. (Paris) 41, C8-437 (1980).
[25]M. Chodorow, Phys. Rev. 55, 675 (1939).
[26]B. Segall, Phys. Rev. 125, 109 (1962).
[27]J. Hubbard, Proc. R. Soc. London Ser. A 281, 401 (1964).
[28]B. Velicky, S. Kirkpatrick, and H. Ehrenreich, Phys. Rev. 175, 747 (1968).
[29]W. L. Johnson, *Glassy Metals I,* Vol. 46 of *Topics in Applied Physics,* edited by H. Beck and H. J. Guntherodt (Springer, Berlin, 1981).
[30]P. W. Anderson, Phys. Rev. 124, 41 (1961).
[31]A. A. Abrikosov and L. P. Gorkov, Zh. Eksp. Teor. Fiz. 39, 1781 (1960) [Sov. Phys.—JETP 12, 1243 (1961)].
[32]S. T. Hopkins and W. L. Johnson, Solid State Commun. 43, 537 (1982).
[33]W. L. Johnson, S. J. Poon, J. Durand, and Pol Duwez, Phys. Rev. B 18, 206 (1978).
[34]W. L. Johnson and K. Samwer (unpublished).
[35]M. Tenhover, J. of Non-Cryst. Solids 44, 85 (1981).
[36]M. Tenhover and W. L. Johnson (unpublished).